Solid State Phenomena Vols. 156-158 (2010) pp 283-288 *Online: 2009-10-28*
© (2010) Trans Tech Publications, Switzerland
doi:10.4028/www.scientific.net/SSP.156-158.283

Electronic States of Oxygen-free Dislocation Networks Produced by Direct Bonding of Silicon Wafers

M. Trushin[1,a], O. Vyvenko[1,2,b], T. Mchedlidze[1,c], O. Kononchuk[3] and M. Kittler[1,4]

[1] IHP/BTU Joint Lab, Konrad-Wachsmann-Allee 1, 03046 Cottbus, Germany

[2] V. A. Fok Institute of Physics, St. Petersburg State University, Ulyanovskaya 1, 108594 St. Petersburg, Russia

[3] SOITEC, Parc des Fontaines, F-38560 Bernin, France

[4] IHP microelectronics, Im Technologiepark 25, 15236 Frankfurt (Oder), Germany

[a] trushmax@tu-cottbus.de, [b] vyvenko@gmail.com, [c] teimuraz.mtchedlidze@tu-cottbus.de

Keywords: Dislocation networks, electronic states of dislocations, DLTS, Pool-Frenkel effect, photoluminescence

Abstract. The results of experimental investigations of the dislocation-related DLTS-peaks originated from the dislocation networks (DN) are presented. Samples with DNs were produced by direct bonding of p-type silicon wafers and no enhancement of oxygen concentration was detected near the DN plane. Origins of the DLTS peaks were proposed and a correlation with the dislocation-related photoluminescence data was established based on known dislocation structure of the samples. Two types of shallow DLTS peaks exhibited Pool-Frenkel effect, which could be linked to the dislocation deformation potential. One of the shallow DLTS peaks was related to straight parts of screw dislocations and another - to the intersections of the dislocations.

Introduction

The dislocation networks (DN) produced by the direct bonding of silicon wafers recently attract an increasing interest due to their potential application in microelectronics as effective light emitters and as perfect conductors (for review see [1]). On the other hand, the DN with the structure pre-determined by the bonding conditions could be used as a model for deeper understanding of properties of dislocations in silicon. Indeed, the density and the types of dislocations in DN are well defined by a misorientation of the surfaces, i.e. by twist and tilt angles between the bonded wafers.

For the case of the investigations by means of deep-level transient spectroscopy (DLTS) method, DNs have special advantages in comparison with the samples containing randomly distributed dislocations (see e.g. [2] and references therein): (i) the DN is strictly parallel to the sample surface; (ii) the distance between the DN and the sample surface can be controlled. Therefore, in combination with the known structure of DN these allow straightforwardly interpret DLTS-results and compare them with the data obtained by other experimental methods, such as photoluminescence.

In previous reports the investigated samples contained large density of oxide precipitates ("oxide islands") at the bonding interface besides the DN itself (see [1] and references therein). The presence of the precipitates complicated investigation of DN properties due to their influence on the electro-physical properties of the material. The experimental results reported in the present work were obtained on the samples where the oxygen concentration at the DN was the same as in the bulk and where the oxide precipitates were not detected by transmission electron microscopy (TEM).

Samples and experimental

Samples were fabricated by direct bonding of 200 mm p-type Si wafers (WB) with (001) surface orientations in hydrophilic process, i.e. the surfaces of the wafers were covered with native oxide layer before the bonding process [3]. Doping level of the wafers was ~10^{15} atoms/cm^3 of boron. Detailed description of the bonding procedure can be found elsewhere [3-5]. After the bonding and a thinning procedure of the top layer, a dislocation network was located at the depth of 170 nm from the sample surface. In order to dissolve the interfacial native oxide layer (INOL), samples were annealed at 1200°C in high purity conditions [3]. After the annealing SIMS investigations did not reveal any variations of oxygen concentration near to the bonding interface.

Wafers were bonded with different twist angles (α_{TW}). A small tilt angle (α_{TI}, ~0.5°) was a result of non-uniformity of wafers polishing. Exact values of tilt and twist angles were defined from X-ray diffraction measurements. The average distance between dislocations in the network as a function of the misorientation angle can be estimated according to the expression [5]:

$$d \sim b / \sin \vartheta , \quad (1)$$

where b is the Burgers vector of a dislocations and ϑ is the misorientation angle. For the dislocations in Si, b = a/2 <110> holds with a = 0.543 nm. The characteristics of the investigated DNs with distances between screw and edge dislocations as well as their average densities calculated from Eq. 1 are presented in Table 1. It should be noted that while a good correspondence between the distances calculated from Eq. 1 and TEM data was found for the small, i.e. 1-3°, misorientation angles, application of Eq. 1 for the larger angles (6° and 30° in our case) is ambiguous due to disturbances of dislocation network caused by the overlapping of the dislocation strain fields.

To produce Schottky contacts for DLTS measurements, 100 nm-thick titanium dots with 1.5 mm diameter were evaporated on the oxide free front surface of all samples. Ohmic contacts were prepared by rubbing of InGa on the rear side of the samples. DLTS measurements were performed by means of transient Fourier spectroscopy system DL-8000 (Accent). Principles of the method and the system can be found elsewhere [6].

Photoluminescence was excited by an Ar-ion laser emitting at 514 nm wavelength with excitation power of 100 mW and the beam was focused to a spot of 100 μm in diameter. The excitation beam was chopped at ~30 Hz frequency for lock-in detection. The emitted light was analyzed with a monochromator and detected by a liquid-nitrogen cooled Ge detector system. More details about PL measurements on these samples can be found elsewhere [7].

Sample	α_{TW}	α_{TI}	D_{SC} 10^6 cm^{-1}	D_{ED} 10^6 cm^{-1}	D_{tot} 10^6 cm^{-1}	d_{SC} nm	d_{ED} nm
L1	1°	0.54°	0.46	0.25	0.71	22	41
L2	3°	0.5°	1.4	0.22	1.62	7.3	44
L3	5.8°	0.67°	2.6	0.31	2.91	3.8	33
L4	29.9°	0.45°	13.4	0.2	13.6	0.7	49

Table 1. Abbreviation used: α_{TW}, α_{TI} - the twist and tilt misorientation angles; D_{SC}, D_{ED}, D_{tot} -densities of screw, edge dislocations and their sum; d_{SC}, d_{ED} - average distances between screw and edge dislocations.

Results and Discussion

PL measurements. PL spectra measured from the samples are presented in Fig.1. The strongest dislocation related luminescence (DRL) spectra consisting mainly of D1 peak at ~0.8 eV was observed from L2 sample. D1 peak was less intensive in L1 sample and was under detection limits in L3 and L4 samples. Extremely weak DRL (mainly D2 and D3 peaks) was found in L3 sample.

Band-to-band (BB) luminescence showed non-monotonic behavior as a function of the twist angle. It was found to be the maximal in L4 sample. Detailed description of PL results for the samples and their interpretation can be found elsewhere [7].

DLTS results. Examples of the DLTS spectra obtained on L1-L4 samples are shown in Fig. 2. DLTS signal-profiling measurements revealed that the origin of the signal in the entire temperature region was located within a narrow region near to the sample surface. An example of such profiling is presented in Fig. 3. In the case under consideration the distribution of the traps is two-dimensional and the relation between the surface density of emitted holes, p_s, and the DLTS signal, dC, is given by:

$$p_s = -\frac{A^2\varepsilon^2}{x_d} eN_A \frac{dC}{C^3}, \qquad (2)$$

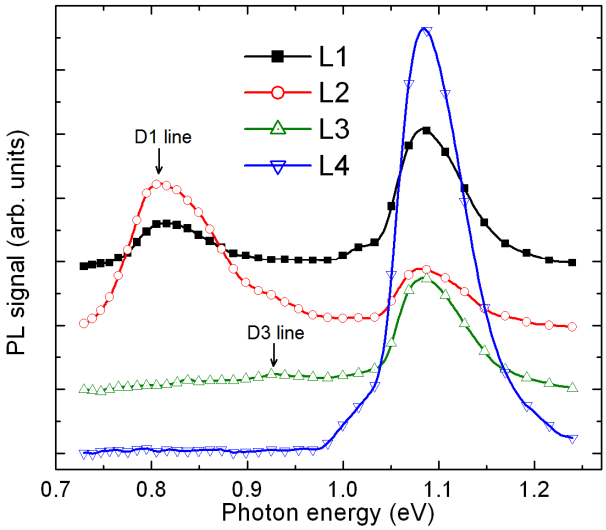

Figure 1. PL spectra detected from L1-L4 samples at 300 K and at 200 mW excitation power. Assignments of the curves are shown in legend.

where ε is dielectric constant, e is elemental charge, x_d is the depth of the dislocation network, C is the diode capacitance, A is the diode area and N_A is the net shallow acceptor density. To account for the Eq. 2, the DLTS signals presented below are normalized to C^3- value.

The low twist-angle samples L1 and L2 showed similar features in DLTS spectra (Fig. 2, left): a low temperature peak and a set of unresolved peaks at 100-250K. The maximum of the main peak in L1 sample, labeled as SL in Fig. 2, is located at a temperature which is 10 K lower than that for the peak QD in L2 sample. Careful examination of the DLTS spectrum of L1 sample reveals that the high temperature side of SL peak has a shoulder just at the position of the QD peak indicating that the QD peak is also presented in the spectrum of L1 sample (see also Fig. 4). The ratio of the magnitudes of the QD peak in L1 and L2 samples is approximately 1:10.

The part of L1 and L2 DLTS spectra between 100 K and 250 K is composed of a set of at least four peaks with the similar or close positions of maximums on temperature scale for both samples.

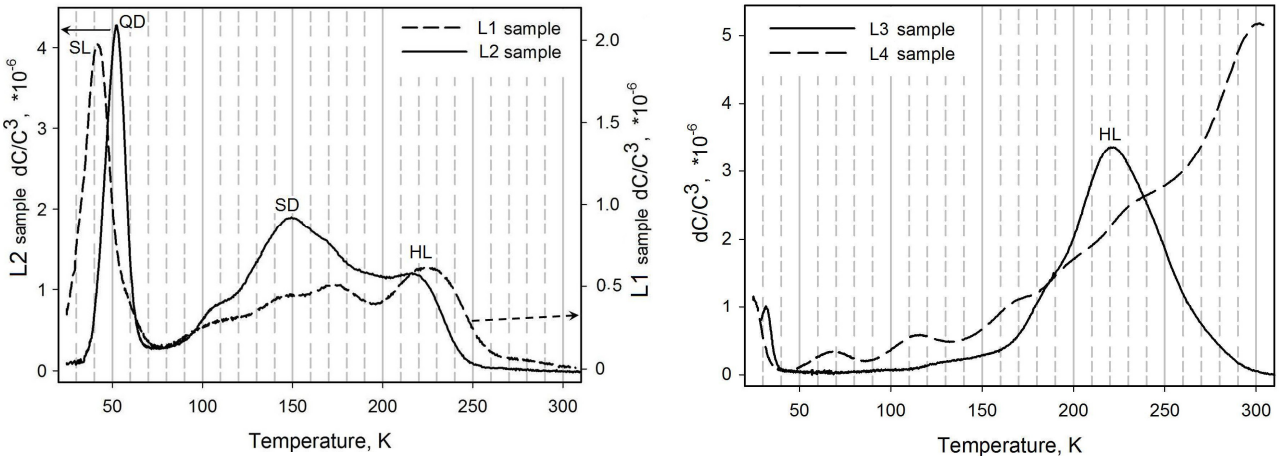

Figure 2. DLTS spectra of L1 and L2 samples (left), and of L3 and L4 samples (right). DLTS-scan parameters: filling pulse duration t_p=100μs, reverse bias U_b=1V, filling pulse voltage U_p= –1V, rate window t_w=20ms. Note different vertical axis scales for the curves in the left figure.

The main difference in the spectrum in this temperature region is the enhancement of the magnitude of the peak marked as SD with the increase of the twist angle from 1° to 3°. Unfortunately, strong overlapping of the peaks complicates determination of their emission characteristics.

DLTS spectra of the large twist-angle samples L3 and L4 differ significantly from that of the low twist-angle samples L1-L2 (see Fig. 2, right). The main feature of DLTS spectrum of L3 sample is an unresolved peak HL, located at around 220 K that could be also recognized in the spectra of L1 and L2 samples. The magnitude of this peak increases with the twist angle. The spectrum for L4 sample shows a set of overlapping DLTS peaks with continuously growing magnitude up to 300 K. The positions of low temperature peaks in L3 and L4 samples are shifted to the lower temperatures with respect to the position of SL and QD peaks in L1-L2 samples and are close to the temperature of freeze-out of shallow acceptors.

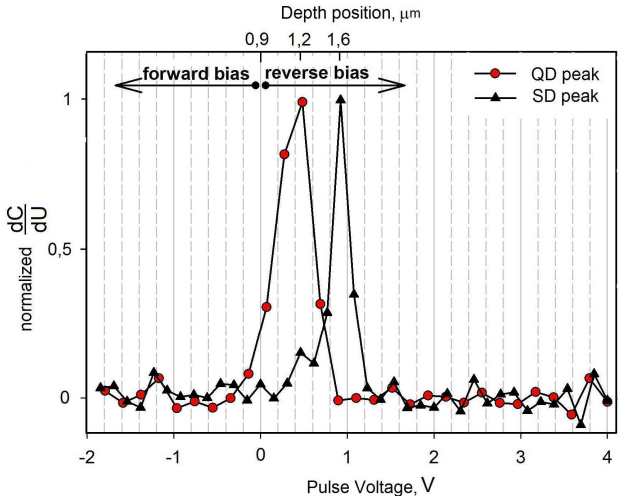

Figure 3. Traps density profiles normalized to their maximum value derived from the refilling pulse voltage dependence of the magnitude of DLTS peaks at T=53 K (QD peak) and at T=150K (SD-peak) in the sample L2. The voltage difference of the profile peaks (~0.4 V) is due the difference of the energetic level positions in band gap. Applied bias voltage was U_b=5 V.

Traps density profiles calculated as the derivative of the dependence of the DLTS signal on the refilling pulse voltage are presented in Fig. 3. The width of the profile peaks is very close to the Debye screening length in the investigated samples, reflecting "plane-like" distribution of the traps. The depth scale at the top Fig. 3 corresponds to the depletion region width, calculated from the stationary capacitance values. The approximation of the depth position of the trap plane, calculated conventionally from the trap energy level and the doping concentration [8] gives the value of ~ 700 nm that is significantly larger than the thickness of the top layer before the thermal treatment, i.e. 170 nm. The reason of this discrepancy is under investigation. As a supposition we could propose a local drop of the hole potential at the interface.

Pool-Frenkel effect. It was found that SL and QD peak positions detected in L1 and L2 samples were shifted toward the lower temperatures with the increase of applied reverse bias, i.e. with the increase of the electric field in the depletion region (see Fig. 4). Detailed examination of the shapes of DLTS peaks and their changes under bias voltage variation confirmed that DLTS signal was composed mainly from two broadened peaks SL and QD.

The activation enthalpies for the hole thermo-emission ΔE_a calculated from the Arrhenius plots at various reverse bias voltages as a function of electrical field followed Pool-Frenkel law for the both levels (see Fig. 5). The dependences could be approximated by expressions:

$$\Delta E_a(\mathrm{QD}) = 0.12 - 2.45\text{e-}4 \sqrt{E(V/cm)} \quad (3)$$

and

$$\Delta E_a(\mathrm{SL}) = 0.13 - 3.78\text{e-}4 \sqrt{E(V/cm)} \quad (4)$$

for QD and SL peaks consequently, giving practically the same value of the trap level position in the bandgap at zero field but showing different slopes.

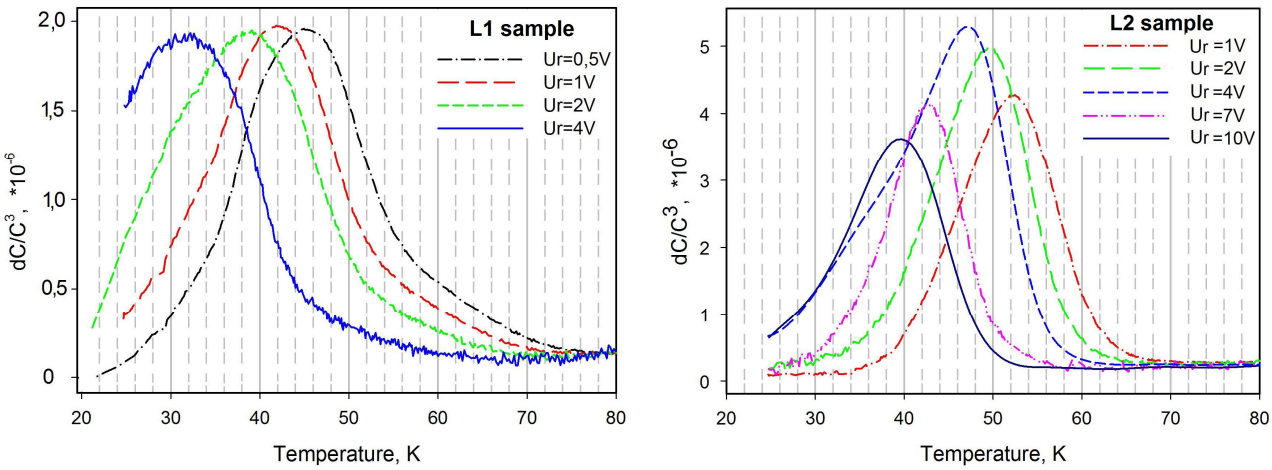

Figure 4. Low temperature part of DLTS spectra of L1 sample (left) and L2 sample (right) measured with different reverse bias voltages. DLTS-scan parameters: filling pulse duration t_p=100μs, filling pulse voltage U_p= –1V, rate window t_w=20ms, reverse bias voltages U_r are shown in the legends.

Possible origins of the DLTS peaks

The magnitude of the SD-peak in L2 sample was approximately three times larger than that in L1 sample, correlating with a threefold larger density of screw dislocations in L2 sample in comparison with L1. The ratio of the magnitudes of QD-peaks between L1 and L2 samples was of about ten, i.e. was equal to square of the screw dislocation density ratio between the samples. From this correlation we can suppose, that SD and SL peaks are related to regular segments of screw dislocations while QD-peak is related to intersections of screw dislocations.

The presence of Pool-Frenkel-like dependence for ΔE_a(E) indicates that the defects responsible for QD and SL DLTS-peaks exhibit an attractive potential for the holes that is inversely proportional to the distance from the trap. According to the theory [8, 9], the pre-factor of the field dependence for the Coulomb potential increases from 1.1e-4 $V^{-1/2}cm^{1/2}$ for three-dimensional (3D) case to 4.4e-4 $V^{-1/2}cm^{1/2}$ for one-dimensional (1D) case. Previously reported pre-factor values for the impurities with the Coulomb potential (see [9] and references therein) were close to the theoretical value for 3D case. The fact that pre-factor values found in this work for SL and QD levels are significantly larger than the later can be explained by a non-Coulombic origin of the potential. We suggest this could be due to a deformation potential of a dislocation that is also inversely proportional to the distance from its core.

The difference between the pre-factor values for SL and QD levels can be explained then to be due to the different dimensionality of the potential within the regular dislocation segments and of intersections of the dislocations. The intersections can be considered as a kind of quantum dots (QD – quantum dot) that have higher dimensionality of its potential (3D) and, accordingly, a lower pre-factor value than the 2D regular dislocation segments. That is in accordance with the suppositions made above.

The zero-field values of the activation energy for the hole emission from SL and QD levels is noticeably larger than that calculated theoretically for the shallow hole states, confined in deformation potential of

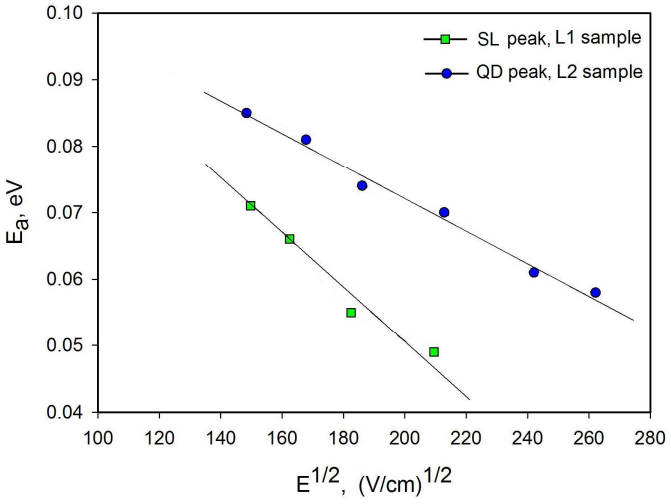

Figure 5. Activation energies for hole thermo-emission from SL and QD traps versus square root of the electrical field in the structure.

screw dislocation (47 meV) [10] and observed experimentally (70 meV) in plastically deformed samples [11]. Accordingly, these levels could originate from the some defects in the dislocation core that are neutral in the empty state. Another possibility is that the states of individual dislocations become deeper due to the effect of the overlapping of their strain fields. Theoretical calculations of the deformation potential levels of the dislocations within a dense dislocation network and of Pool-Frenkel effect for dislocation deformation potential are necessary to clarify this problem.

A correlation could be seen between PL and DLTS results for the L1 and L2 samples. The magnitudes of SL and SD DLTS-peaks and the intensity of D1 peak in PL spectra have similar differences between L1 and L2 samples indicating that all that features are related to the same kind of dislocation related defects. Moreover, shallow levels dominating in these samples can not serve as an effective channel for non-radiative recombination, but rather might be the levels responsible for D1 luminescence.

With the increasing of the twist angle to 6° and further to 30°, defects having deep levels become dominating in DLTS-spectra and that is accompanied with the drastic reduction of DRL D1 peak. The reduction of D1 is not related to increase of the non-radiative recombination, since the enhancement of BB luminescence was observed in these samples, see Fig. 1 and [7]. On the other hand, the density of the edge dislocations is practically the same in all our samples (see Table 1), thus redistribution of DRL could not be the reason as well. Therefore, the possible reason of the changes in the trap level content and of the disappearance of DRL should be a destruction of specific structures in the core of screw dislocations that give rise to D1 DRL. As a further confirmation of cardinal changes in the DN structure with increase in the twist angle could be the correspondence of the energy distribution of hole trap states observed in L4 sample with that known for large angle grain boundaries [12]. Similar distribution was attributed in [12] to defects possessing deep levels in the bandgap, formed or segregated due to the large lattice mismatch.

References

[1] M. Kittler, X. Yu, T. Mchedlidze, T. Arguirov, O. Vyvenko and W. Seifert, M. Reiche, T. Wilhelm, M. Seibt, O. Voss, W. Fritzsche, A. Wolff, Small, Vol. 3 (2007), p. 964.

[2] W. Schröter, H. Hedemann, V. Kveder and F. Riedel, J. Phys.: Condens. Matter, Vol. 14 (2002), p. 13047.

[3] O. Kononchuk, F. Boedt and F. Allibert, Sol. St. Phenom., Vol. 131-133 (2008), p.113.

[4] M. Reiche, Mat. Sci. Forum, Vol. 590 (2008), p.57.

[5] T. Wilhelm, T. Mchedlidze, X. Yu, T. Arguirov, M. Kittler and M. Reiche, Sol. St. Phenom., Vol. 131-133 (2008), p. 571.

[6] S. Weiss and R. Kassing, Solid-State Electronics, Vol. 31 (1988), p. 1733.

[7] T. Mchedlidze, O. Kononchuk, T. Arguirov, M. Trushin, M. Reiche and M. Kittler, proceedings of this conference, GADEST 2009.

[8] P. Blood and J. W. Orton, *The electrical characterization of semiconductors: majority carriers and electron states*. 1992, London: Academic Press.

[9] P.A. Martin, B.G. Streetman, K.Hess, J. Appl. Phys., Vol. 52 (1981), p. 7409.

[10] J.-L. Farvacque and P. Francois, Phys. Stat. Sol. (b), Vol. 223 (2001), p. 635.

[11] A. Castaldini, D. Cavalcoli, A.Cavallini, S. Pizzini, Phys. Rev. Lett., Vol. 95 (2005), p. 076401.

[12] G. C. McGonigal, D. J. Thomson, J. G. Shaw and H. C. Card, Phys. Rev. B, Vol. 28 (1983), p. 5908.

Gettering and Defect Engineering in Semiconductor Technology XIII
10.4028/www.scientific.net/SSP.156-158

Electronic States of Oxygen-Free Dislocation Networks Produced by Direct Bonding of Silicon Wafers
10.4028/www.scientific.net/SSP.156-158.283

DOI References

[1] M. Kittler, X. Yu, T. Mchedlidze, T. Arguirov, O. Vyvenko and W. Seifert, M. Reiche, T. Wilhelm, M. Seibt, O. Voss, W. Fritzsche, A. Wolff, Small, Vol. 3 (2007), p. 964.
doi:10.1002/smll.200600539
[2] W. Schröter, H. Hedemann, V. Kveder and F. Riedel, J. Phys.: Condens. Matter, Vol. 14 (2002), p. 13047.
doi:10.1088/0953-8984/14/48/350
[5] T. Wilhelm, T. Mchedlidze, X. Yu, T. Arguirov, M. Kittler and M. Reiche, Sol. St. Phenom., Vol. 131-133 (2008), p. 571.
doi:10.4028/www.scientific.net/SSP.131-133.571
[7] T. Mchedlidze, O. Kononchuk, T. Arguirov, M. Trushin, M. Reiche and M. Kittler, proceedings of this conference, GADEST 2009.
doi:10.4028/www.scientific.net/SSP.156-158.567
[11] A. Castaldini, D. Cavalcoli, A.Cavallini, S. Pizzini, Phys. Rev. Lett., Vol. 95 (2005), p. 076401.
doi:10.1103/PhysRevLett.95.076401
[12] G. C. McGonigal, D. J. Thomson, J. G. Shaw and H. C. Card, Phys. Rev. B, Vol. 28 (1983), p. 5908.
doi:10.1103/PhysRevB.28.5908
[4] M. Reiche, Mat. Sci. Forum, Vol. 590 (2008), p.57.
doi:10.4028/www.scientific.net/MSF.590.57
[6] S. Weiss and R. Kassing, Solid-State Electronics, Vol. 31 (1988), p. 1733.
doi:10.1016/0038-1101(88)90071-8
[11] A. Castaldini, D. Cavalcoli, A.Cavallini, S. Pizzini, Phys. Rev. Lett., Vol. 95 (2005), p. 76401.
doi:10.1002/pssa.200460510
[12] G. C. McGonigal, D. J. Thomson, J. G. Shaw and H. C. Card, Phys. Rev. B, Vol. 28 (1983), p. 908.
doi:10.1103/PhysRevB.28.5908